EARTH SCIENCES
RESEARCH JOURNAL
Earth Sci. Res. J. Vol. 29, No. 2 (June, 2025): 131 - 137

UNIVERSIDAD NACIONAL DE COLOMBIA

GEOLOGY

Evidence of fluid process for Li-Rb-F-W rich vein rocks of Degana, Rajasthan, India

Vijay Anand, S*, Nisha Devi, R
Department of Applied Sciences (Applied Geology), Curtin University, Miri-98009, Sarawak, Malaysia
*Corresponding email: vijay.anand@curtin.edu.my

ABSTRACT

Several mineralized vein rocks were intruded into the granites of Rajasthan, India. In some of the vein rocks in Rajasthan has associated with enormous amount of critical metals and rare metals. The metals are spatially associated with the vein rocks of Degana, Rajasthan, India. Six samples were collected in wall and core of the vein rocks. Two samples from wall and one sample from core of each vein respectively. The samples were selected for fluid inclusion and laser Raman microprobe studies. Four distinct types of fluid inclusion were identified and classified. Type I is aqueous bi-phase ($L_{H2O}+V_{H2O}$) inclusion; Type II is aqueous-carbonic ($L_{H2O}+L_{CO2}$) inclusion; Type III is carbonic mono liquid (L_{CO2}) inclusion under room temperature; Type IV is polyphase inclusion ($L_{H2O}+V_{H2O}+S$). The varying homogenization temperatures with different salinities implies mixed fluid process. The fluid process was mainly derived from the host rock granite. Later the cooled magmatic fluids were mixed with the meteoric water during hydrothermal stage may be the major key factor for formation of Li-Rb-F-W mineralization in Rajasthan, India.

Keywords: Neoproterozoic; vein rock; fluid salinity; fluid boiling; carbonic inclusion; Laser Raman microprobe.

Evidencia de un proceso fluido en rocas veteadas ricas en Li-Rb-F-W de Degana, Rajastán, India

RESUMEN

Varias vetas de roca mineralizadas fueron intruidas en los granitos de Rajastán, India. Algunas de estas vetas de Rajastán presentan una enorme cantidad de metales críticos y raros. Estos metales están asociados espacialmente con las vetas de Degana, Rajastán, India. Para este trabajo se recolectaron seis muestras de la pared y del núcleo de dos vetas. Dos muestras de la pared y una del núcleo de cada veta, respectivamente. Las muestras se seleccionaron para estudios de inclusión fluida y microsonda láser Raman. Se identificaron y clasificaron cuatro tipos distintos de inclusión fluida: el tipo I es una inclusión acuosa bifásica ($L_{H2O}+V_{H2O}$); el tipo II es una inclusión acuoso-carbónica ($L_{H2O}+L_{CO2}$); el tipo III es una inclusión carbónica monolíquida (L_{CO_2}) a temperatura ambiente; y el tipo IV es una inclusión polifásica ($L_{H2O}+V_{H2O}+S$). La variación en las temperaturas de homogeneización con diferentes salinidades implica un proceso de fluido mixto. Este proceso fluido se derivó principalmente del granito de la roca huésped. Más tarde, los fluidos magmáticos enfriados se mezclaron con el agua meteórica durante la etapa hidrotermal, lo que puede ser el principal factor clave para la formación de la mineralización de Li-Rb-F-W en Rajastán, India.

Palabras clave: neoproterozoico; veta de roca; salinidad del fluido; lava; inclusión carbónica; microsonda láser Raman.

Record
Manuscript received: 03/04/2024
Accepted for publication: 13/03/2025

How to cite this item:
Anand, V. S., & Devi, N. R. (2025). Evidence of fluid process for Li-Rb-F-W rich vein rocks of Degana, Rajasthan, India. *Earth Sciences Research Journal*, 29(2), 131-137. https://doi.org/10.15446/esrj.v28n2.113775

ISSN 1794-6190 e-ISSN 2339-3459
https://doi.org/10.15446/esrj.v28n2.113775

1. Introduction

Lithium (Li), rubidium (Rb), and tungsten (W) are economically valuable critical metals and widely used into many industrial applications (Wang et al., 2017b; Huang et al., 2020; Sovacool et al., 2020; Xu et al., 2021; Deng et al., 2022; Guo et al., 2022; 2023; Wenkai et al., 2023). The critical metals are often associated with many magmatic and hydrothermal vein rocks in different geodynamic settings (Linnen et al., 2012; Kaeter et al., 2018; Liu et al., 2020; Yin et al., 2020). The hydrothermal vein rocks are broad diversity of economic interest, and it is a significant source for many metals. Understanding the metallogenesis by SIMS (Secondary Ion Mass Spectrometry), ICP-MS (Inductively Coupled Plasma Mass Spectrometry), and SHRIMP (Sensitive High-Resolution Ion Microprobe) have been used significantly (Li et al., 2023; Xu et al., 2023).

In India, Rajasthan characterized by many granitic rocks and intruded by many hydrothermal vein rocks and enriched with Li, Rb, W, Sn, B, Nb and Ta (Chattopadhyay et al., 1994; Pandian, 1999; Pandian and Varma, 2001; Singh and Singh, 2001). In Rajasthan, Degana region has well occupied three important mineralized hills (Phyllite hill, Tikli hill, and Rewat hill) (Figure 1). Several mineralized vein rocks are intruded into the granites of Degana, Rajasthan, India (Pandian and Varma, 2001). In Tikli hill, the mineralized vein rock is approx. 30-40cms wide and >1meter long and has the trend of N29° with moderate dip (18º). Similarly, In Rewat hill, the mineralized vein rock is approx. 50cm wide and >1.5meter long. The mineral assemblages and the grain sizes may vary from wall to core of the vein. Anand et al., 2018 has reported about the Degana granite (greisen quartz) associated tungsten deposit fluid process. Till now no one reported about the wall-core vein rock fluid characteristics; In this manuscript reporting the types of fluid inclusions, fluid composition, fluid salinity, first melting temperature, last ice melting temperature, clathrate (gas hydrate) melting temperature and homogenization temperatures to elucidate the fluid process are discussed in this manuscript.

2. Methodology

Six samples were obtained from the Tikli and Rewat granite intruded mineralized vein rocks. Two of the samples were collected from western and eastern wall of the vein, one sample from the quartz rich core (quartz-zinnwaldite) respectively. The doubly polished thin wafer sections of these Li-Rb-F-W samples were prepared for microscopic studies.

2.1 Fluid-microthermometry

The fluid-microthermometry (heating-freezing) were measured by Linkam THMS-600 stage mounted on the Leica transmission microscope (German made). The unit were operating in the temperature range is -180 to +600ºC (L(liquid) N(nitrogen) T(temperature). The fluid-microthermometry unit calibrated by using synthetic CO_2-H_2O inclusion (CO_2 triple point (-56.6 ºC) and H_2O triple point (-0.01 ºC). The inclusions were freezes to -100ºC for solidification and warmed slowly. The Type I to Type III inclusions were cooled first until solidified, then heated slowly to record CO_2 and H_2O melting temperature (triple points), clathrate melting temperature, and homogenization temperature. Type IV inclusions were heated (10ºC/min) to record the liquid-vapor (L-V) homogenization temperature (Th_{H2O}) and salt dissolution temperature (Tm_{salt}). Data generated on only those inclusions not decrepitated and gave reproducible during the freezing-heating runs. The doubly polished wafer sections were prepared and analyzed at the Department of Earth Sciences, Pondicherry University, India and Curtin University, Malaysia. The measurement accuracy is ±0.2ºC during freezing and ±2ºC during heating runs. The detailed Tikli and Rewat vein rocks fluid inclusion data were given in the Table 1-4.

3. Results

3.1 Vein rock petrography

Tikli and Rewat vein rocks mainly composed of k-feldspar, zinnwaldite (Li-mica), plagioclase, quartz and topaz phenocrysts in a fine-grained matrix (groundmass) (Figure 3). The matrix predominantly composed of feldspar and quartz. The feldspar and quartz phenocrysts are corroded along their margins by the surrounding matrix phase. Quartz is partially reabsorbed (replacement) by k-feldspar (Figure 3c). The zinnwaldite shows the colorless to slightly darker colored, which shows the strong pleochroism and light brown to orange-blue interference colour. The zinnwaldite grains were typically associated with quartz and feldspar in the wall of the vein rock (Figure 2 and 3).

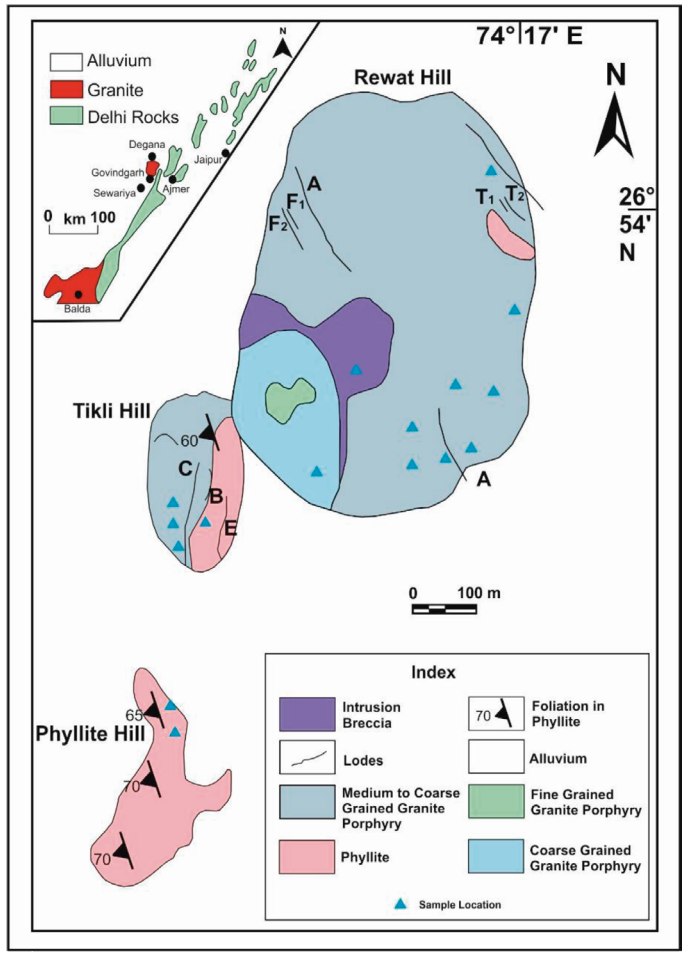

Figure 1. Geological map of Degana hill (Phyllite hill, Tikli hill, Rewat hill), Rajasthan, NW India (modified after Anand et al., 2018).

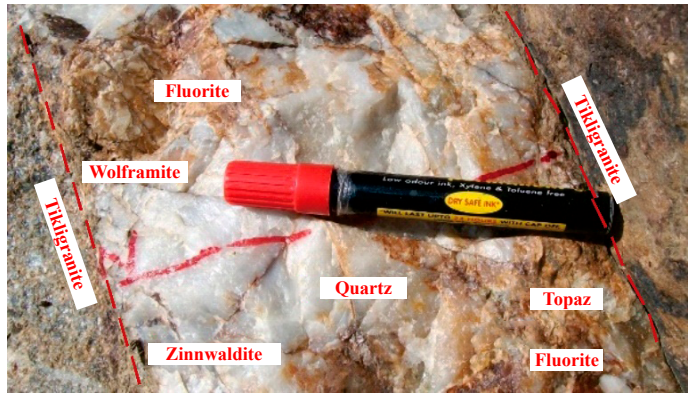

Figure 2 (a) Li-Rb-F-W mineralized vein rock intruded into Tikli granite, Degana, Rajasthan, NW India.

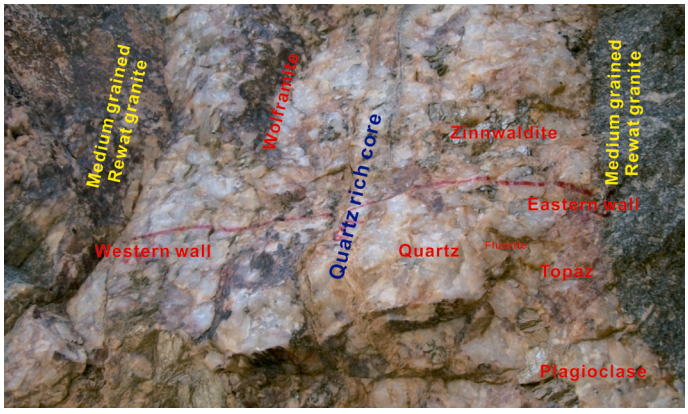

Figure 2(b) Li-Rb-F-W mineralized vein rock intruded into Rewat granite, Degana, Rajasthan, NW India.

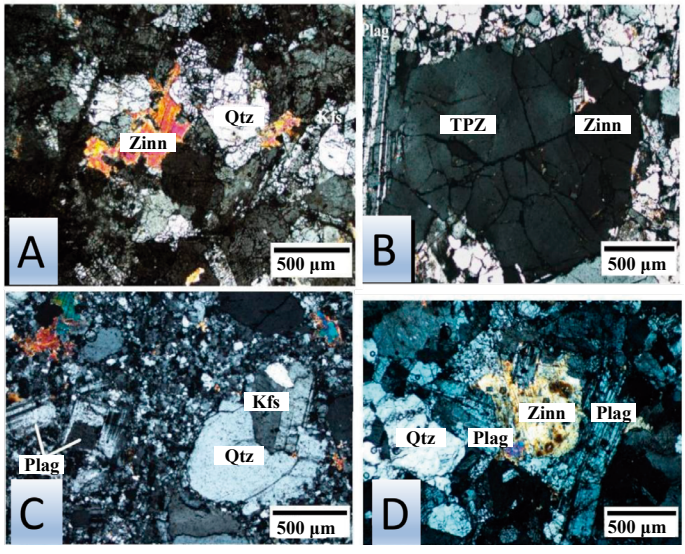

Figure 3. Microphotographs of Li-Rb-F-W mineralized quartz vein rock samples. (A-B) Tikli vein rock; (C-D) Rewat vein rock. Mineral abbreviations: **Qtz**-Quartz; **Plag**-Plagioclase feldspar; **Kfs**-K-feldspar; **Tpz**-Topaz; **Zinn**-Zinnwaldite.

3.2 Fluid Inclusion in Li-Rb-F-W mineralized vein rock

Fluid inclusion in vein rock samples were genetically classified into primary inclusions (isolated and group of inclusions), secondary (intergranular) and pseudo-secondary (intra granular) inclusions (planar arrays or trails) (Shepherd et al. 1985, Roedder,1992, Bakker, 2003, Bodnar et al., 2014). Secondary and Pseudo-secondary inclusion not focused for the present study. Fluid inclusions were not recorded for feldspar, topaz minerals due to poor anisotropism contrast with quartz mineral. Few aqueous inclusions were observed in zinnwaldite, due to its contrasting light intensity unable to run microthermometry. Four types of inclusions were classified in quartz-zinnwaldite minerals contact zone. **Type I** is aqueous bi-phase (L_{H2O}+V_{H2O}) inclusions; **Type II** is aqueous-carbonic inclusions (L_{H2O}+L_{CO2}) with graphite (C). The size of the inclusion varies from 8 to 20µm, and the shape is almost oval to rounded and irregular. **Type III** is carbonic monophasic inclusion, which contains CO_2 liquid (L_{CO2}) at ambient laboratory temperature. **Type IV** is polyphase inclusion (L_{H2O}+V_{H2O}+C+S_1+S_2). **Type IV** inclusions were randomly distributed with size ranging from 4-16µm, and the shape is irregular, rectangular, and rounded (Figure 4-5).

3.3 Tikli Li-Rb-F-W mineralized vein rock

The first melting temperature recorded for Type I-III inclusions at -23 to -25°C and -61 to -42°C, suggesting that the solution has mixture of Li^+, K^+, Na^+, Ca^{2+}, F, and Cl^-. The final ice melting temperature varies from -12.4 to -4.3°C (salinity: 16.3 to 6.8 wt. % NaCl equivalent). Type I inclusions were homogenized into liquid between 200-325°C (L_{H2O}>V_{H2O}→ L_{H2O}), while some inclusions were homogenized into vapor between 240-370°C (V_{H2O}>L_{H2O}→V_{H2O}). For Type II inclusions, the Tm_{CO2} recorded between -59.4 and -56.5°C (indicates presence of other volatile phases). Tm-clathrate recorded between 2.5 to 8.6 (salinity: ~16.2 to 4.9 wt. % NaCl equivalent) (Darling, 1991). The partial Th_{CO2} recorded between 20-29°C (L_{H2O}+L_{CO2}>V_{CO2}→L_{H2O}+L_{CO2}) and the Th_{total} for Type III inclusions observed at 200-356°C (L_{H2O}+L_{CO2}→L_{H2O}). Some of the Type II inclusions were homogenized into vapor (275-396°C). For type III inclusions, Tm_{CO2} recorded between -62.3 to -57.0°C (indicates presence of other carbonic phases). The Th_{CO2} of these inclusions were homogenized into vapor phase between 10 and 27°C (V_{CO2}>L_{CO2}→V_{CO2}). For Type IV inclusions, vapor out temperature for Type IV inclusions were occurred between 185-330°C (L_{H2O}>V_{H2O}+S→L_{H2O}+S). The total homogenization observed by the disappearance of salt (salt melting or dissolution) average at 210-386°C (salinity: 32-46 wt. % NaCl equivalent) (Table 1). The fluid salinity calculated based on the last ice melting (Type-I) (Goldstein, 1994), clathrate melting (Type-II-III) (Darling, 1991) and salt melting (dissolution) temperatures (Type IV) (Goldstein, 1994; Bodnar, 1993).

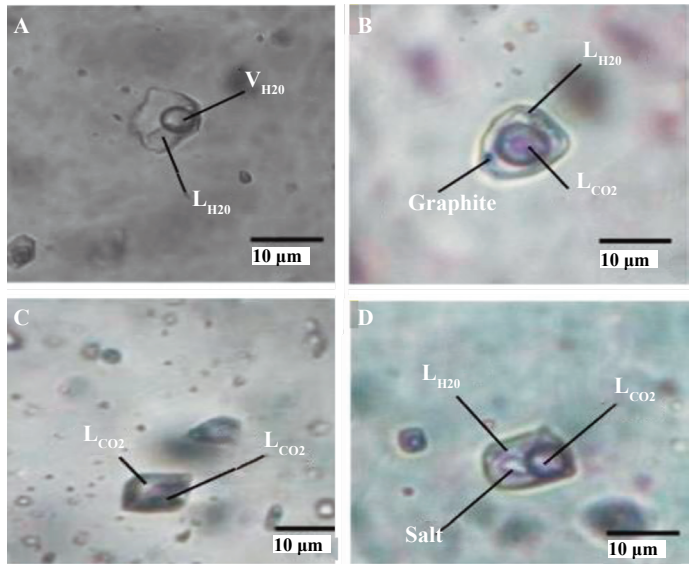

Figure 4: Types of fluid inclusions from Tikli and Rewat granite associated mineralized vein rock samples, Degana, Rajasthan, NW India. (**a**) Type I inclusions; (**b**) Type II inclusions; (**c**) Type III inclusions; (**d**) Type IV inclusions.

3.4 Rewat Li-Rb-F-W mineralized vein rock (wall-core)

The first melting temperature for Type I inclusions for western wall is (-68 and -12°C), core (-62 and -15°C) and eastern wall (-64 and -52°C). The solution has rich in Li^+ Na^+, K^+, Ca^{2+}, and Mg^{2+} in the wall zones, while being richer in Li^+, Na^+, K^+ Ca^{2+} in core of the vein. The final ice melting temperature and salinity varies from western wall (-10.1 to -4.2°C/14 to 6.7 wt. % NaCl equivalent) to core (-4.4 to -1.2°C/7.2 to 2 wt. % NaCl equivalent) and eastern wall (-13.1 to 4.5°C/17 to 7.2wt. % NaCl equivalent). For Type I inclusions, the average homogenization temperature into liquid between (L_{H2O}>V_{H2O}→L_{H2O}), for western wall is 220 to 310°C, core of the vein is 160 to 235°C and eastern wall is 250 to 355°C. Some Type I inclusions were homogenized into a vapor phase between 190-380°C (V_{H2O}>L_{H2O}→V_{H2O}) in the wall zone. For Type II, the Tm_{CO2} was recorded in western wall (-61 to -57°C), core (-64 to -57.6°C),

and eastern wall (-58 to -56.7°C). The clathrate melting temperature for the wall of the vein is (3.1 to 7°C/14.1 to 5.05 wt. % NaCl equivalent); core (6.5 to 8°C/8 to 3 wt. % NaCl equivalent). The partial homogenization for Type II inclusion in wall of the vein is 12-29°C and core of the vein 2-15°C. The total homogenization temperature ($L_{H2O}>L_{CO2}\rightarrow L_{H2O}$) for Type II inclusion in western wall (265-340°C), core of the vein (170 to 225°C) and eastern wall (218-348°C). Some of Type II inclusions were homogenized into vapor ($V_{H2O}>L_{H2O}$) between 245-412°C in wall zones. For Type III inclusions, the Tm_{CO2} was recorded in western wall (-59 to -57.1°C), core (-60 to -56.6°C) and eastern wall (-59 to -56.8°C). The homogenization temperature for Type III inclusion for western wall (15-26°C), eastern wall (12-20°C) and core zone (-2 to 10°C). For Type III inclusions were homogenized into vapor phase. The salt melting (dissolution) temperature for type IV inclusions in western and eastern wall (145 to 412°C; 152 to 385°C (the corresponding salinity range is 29.5-48 wt. % NaCl equivalent). The liquid-vapor homogenization temperature for type IV inclusions in the wall of the vein varies from 138-352°C (western) and is 132-298°C (eastern wall). The Type IV inclusions were not found in the core of the vein (Table 2-4).

4. Laser Raman microprobe

Laser Raman microprobe is an important method to identify the volatile species composition (CO_2, CH_4, C, N_2) of the fluid inclusions. The volatile composition identified based on the Raman shift value of the spectra obtained (Frezzotti et al., 2012). The samples were analyzed by "Thermo Almega Laser XR dispersive Raman Spectrometer, the accumulation time for each scan is ~20-25 secs; 50 and 100x high standard objectives were used for observation in the Department of Earth Sciences, IIT Bombay, India. The volatile composition of CO_2 doublets (1274 & 1378cm^{-1}), graphite (1602cm^{-1}) (D-peak) and CH_4 (2911cm^{-1}) (G-peak) were identified in the mineralized samples (Figure 6).

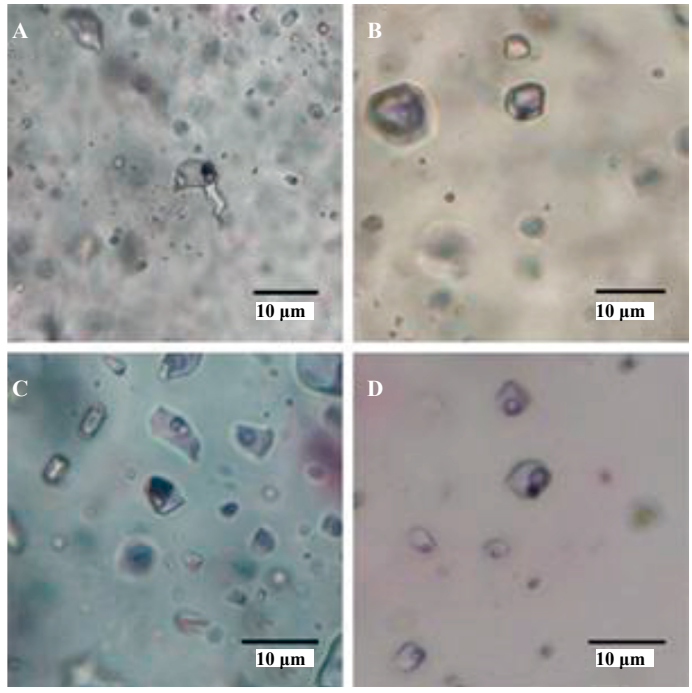

Figure 5. Types of fluid inclusions from Tikli and Rewat granite associated mineralized vein rock samples, Degana, Rajasthan, NW India. (**A-D**) metal rich inclusions.

Table 1. Fluid microthermometry of Tikli mineralized vein rock, Degana, Rajasthan, India

Fluid Type	Phases	Composition	Tm_{CO2} (°C)	Tclath (°C)	Th_{CO2}(°C)	Thtot.(°C)	Teut(°C)	Tmice(°C)	Th_{H2O}(°C)	TmSalt(°C)	Salinity (wt. %)
I	L+V	$L_{H2O}+V_{H2O}$					-23 to -25 -61 to -42	-12.4 to -4.3	200-325 (L) 240-370 (V)		16.3 to 6.8
II	L1+L2+V	$L_{H2O}+L_{CO2}+V_{CO2}$	-59.4 to -56.5	2.5 to 8.6	20-29	200-356(L) 275-396(V)					16.2 to 4.9
III	L	$L_{CO2+}V_{CO2}$	-62.3 to -57.0		10 and 27						
IV	L+V+S	$L_{H2O}+V_{H2O}$+Salt							185-330	210-386	32 to 46

Table 2. Fluid microthermometry of Rewat mineralized vein rock (**western wall**).

Fluid Type	Phases	Composition	Tm_{CO2} (°C)	Tclath (°C)	Th_{CO2}(°C)	Thtot. (°C)	Teut(°C)	Tmice(°C)	Th_{H2O}(°C)	TmSalt(°C)	Salinity (wt. %)
I	L+V	$L_{H2O}+V_{H2O}$					-68 to -12	-10.1 to -4.2°C	220 to 310(L) 190 to 380(V)		14 to 6.7
II	L_1+L_2+V	$L_{H2O}+L_{CO2}+V_{CO2}$	-61 to -57	3.1 to 7	12 to 29	265 to 340 (L) 225 to 412 (V)					14.1 to 5.05
III	L	L_{CO2}	-59 to -57.1		15to 26 (V)						
IV	L+V+S	$L_{H2O}+V_{H2O}$+Solid							138-352	145 to 412	29.5 to 48

Table 3. Fluid microthermometry of Rewat mineralized vein rock (core).

Fluid Type	Phases	Composition	Tm_{CO2}(°C)	Tclath (°C)	Th_{CO2}(°C)	Thtot.(°C)	Teut(°C)	Tmice(°C)	Th_{H2O}(°C)	TmSalt(°C)	Salinity (wt. %)
I	L+V	$L_{H2O}+V_{H2O}$					-62 to -15	-4.4 to -1.2	160 to 235		7.2 to 2
II	L1+L2+V	$L_{H2O}+L_{CO2}+V_{CO2}$	-64 to -57.6	6.5 to 8	2 to 15	170 to 225					8 to 3
III	L	L_{CO2}	-60 to -56.6		12 to 20(V)						

Table 4. Fluid microthermometry of Rewat mineralized vein rock (eastern wall).

Fluid Type	Phases	Composition	Tm_{CO2}(°C)	Tclath (°C)	Th_{CO2}(°C)	Thtot.(°C)	Teut(°C)	Tmice(°C)	Th_{H2O}(°C)	TmSalt(°C)	Salinity (wt. %)
I	L+V	$L_{H2O}+V_{H2O}$					-64 to -52°C	-13.1 to 4.5	250 to 355		17 to 7.2
II	L1+L2+V	$L_{H2O}+L_{CO2}+V_{CO2}$	-58 to -56.7	1.5 to 6.8	20-24	218-348					13 to 6.5
III	L	L_{CO2}	-59 to -56.8		12-20 (V)						
IV	L+V+S	$L_{H2O}+V_{H2O}$+Solid							132-298	152 to 385	30 to 46

Abbreviations: CO_2 melting temperature (**Tm_{CO2}**); Clathrate melting temperature (**Tm_{clath}**); CO_2 homogenization temperature (**Th_{CO2}**); Total homogenization temperature (**Thtot**.); Eutectic (first melting) temperature (**Teut**); H_2O ice melting temperature (**Tmice**); H_2O homogenization temperature (**Th_{CO2}**); Salt melting (**dissolution**) temperature (**Tmsalt**).

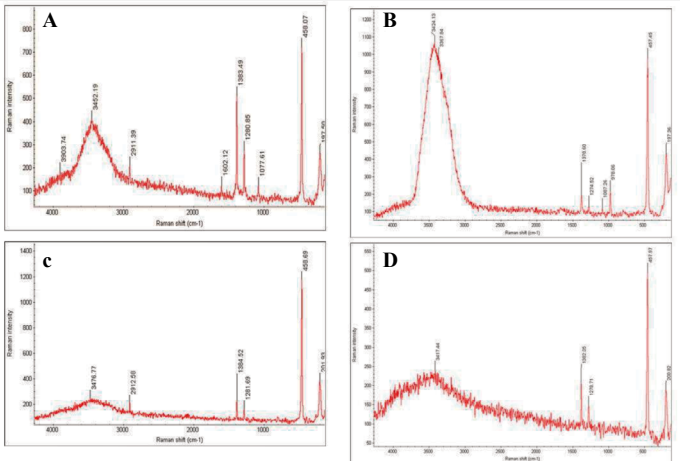

Figure 6. (**a**) Laser Raman microprobe spectra of Type II inclusions (fermi CO_2 doublets at 1280 and 1383cm^{-1}) and H_2O liquid (3452cm^{-1}) in Tikli mineralized vein rock; (**b**): Type II inclusions (fermi CO_2 doublets at 1274 and 1378cm^{-1}), graphite (1602cm^{-1}) and H_2O liquid (3424cm^{-1}) in Rewat mineralized vein rock (western wall); (**c**): Type II (fermi CO_2 doublets at 1281 and 1384cm^{-1}, (CH_4 at 2912 cm^{-1}) inclusions in the Rewat mineralized vein rock (core quartz). (**d**): Type II inclusions (fermi CO_2 doublets at 1278 and 1382cm^{-1}) and H_2O liquid (3417cm^{-1}) in the Rewat mineralized vein rock (eastern wall).

5. Discussion

The Tikli-Rewat granites and the mineralized vein rocks contain significant amount of zinnwaldite (Li rich), plagioclase (Rb-rich), fluorite (F), tourmaline (B), topaz (Al-F) and wolframite (W). In Degana, Li (~4000 ppm), Rb (>1000 ppm), F (4-6 wt. %), W (50 ppm) are above the crustal abundances in the small volume of the study area (Anand et al., 2018; Ghosh et al. 2023), so that it is important to understand the conditions of metals formation. The geochemistry, petrogenesis and geochronology of Degana granites were discussed by several researchers (Pandian and Varma, 2001, Chattopadhyay et al., 1994; Anand et al., 2018; Ghosh et al., 2023; Kumar et al., 2023).

The fluid process of the mineralized wall-core vein rock (magmatic-hydrothermal mineralization) remains unclear in the study area. Understanding the relationship between wall rock granite and intruded mineralized vein rock is crucial for elucidating the metallogenetic mechanism. In the field. the mineralized vein rocks consists of zinnwaldite, fluorite, plagioclase, and topaz are lining the vein wall, and quartz occupies the bulk of the vein rock (Figure 2 a-b). The vein rock intruded into the many fracture plans and filled by various mineral assemblages and finer greisen (altered) veinlets lining the walls, which suggests a genetic linkage between the host rock and mineralization (Figure 2).

The fluid petrography, microthermometry (lowering of melting temperature), and laser Raman microprobe (composition of volatile phases) observation clearly indicates that the mineralized fluid system is interpreted to be H_2O-CO_2-NaCl±CH_4. The Tikli mineralized vein rock samples and Rewat mineralized vein rock samples show different homogenization temperatures and different salinities (Type I-IV inclusion) of 220 to 310°C/265 to 340°C for the western wall, 160 to 235°C/170 to 225°C for the core of the vein, and 250 to 355°C/265 to 342°C for the eastern wall. The corresponding salinities are 14 to 6.7/14.1 to 7.5°C wt. % NaCl equivalent for the western wall, 7.2 to 2/8 to 3 wt. % NaCl equivalent for the core of the vein, and 17 to 7.2/8 to 3 wt. % NaCl equivalent for the eastern wall. The different homogenization temperatures (Type-I to IV) with varying salinities represents a mixed fluid process. Additionally, aqueous bi phase, polyphase and the carbonic fluid inclusions represented by the entrapment with variable phase ratios, presence of graphite (captive phase) and lowering the CO_2 melting temperature (<-56.6°C) are further evidences.

Many fractionated mineralized granites, granitic pegmatites and intruded vein rocks have been identified worldwide, such as Black Hills, South Dakota; Altai and Cuonadong Dome, P.R. China; Damara Belt in Namibia (Shearer et al., 1987; Jolliffe et al., 1987; Yin et al., 2013; Hulsbosch et al., 2014; Kaeter et al., 2018; Liu et al., 2020; Yin et al., 2020; Xie et al., 2020; Bacík et al., 2021). The Degana granites has been argued to be highly fractionated at a higher degree (Pandian and Varma, 2001). Fractional crystallization is to be considered a principal mechanism for the formation of many wall-core zoned Li-Rb-F-W rich deposits (Liu et al., 2020; Yin et al., 2020; Bacík et al., 2021). The fluid process may vary due to mineralization style, wallrock interaction, except for simple cooling process (lack of fluid-wallrock interaction) (Heinrich, 1990, Heinrich et al., 2004; Xie et al., 2019; Li et al., 2019; Zhang et al., 2021; Li et al., 2021). The hot circulation of fluids in the mineralized zone through

fracture planes is mainly controlled by type of inclusions, suggesting these fluids are major source for the vein rocks. The carbonic, aqueous-carbonic and hypersaline inclusions represent a mixture in the mineralized vein rocks during crystallization. The mixing of greisenised wallrock granite (magmatic fluids) and the hydrothermal-derived meteoric fluids (vein rock) carrying high amounts of metals (metal rich inclusion). in to the host rock and the associated vein rocks in Degana, Rajsthan, India

6. Conclusion

As discussed above based on the field evidence, analytical data, we propose that the fluid process of Tikli and Rewat vein rock were mainly derived from Degana granitic magma. The granitic magmatic evolution is highly differentiated in composition. The magmatic fluids (wallrock) carried out a large amount of metal complex flowed through fractures (vein rock) and precipitated the Li, Rb, W rich minerals while temperature reduced (during meteoric stage). Cooling of the metal forming fluids and the meteoric water are the key factors that led to the formation of mineral deposit in the study area.

Acknowledgement

We would like to acknowledge CMRI (Curtin Malaysia Research Institute Malaysia for the financial support for this research work is greatly acknowledged (Grant Number: 006043). The author thankful to the Journal editor and reviewer for the constructive reviews and comments are greatly acknowledged.

Competing interest:

The corresponding author and co-authors declare that there is no conflict of interest.

References

Bakker, R.J (2003). Package FLUIDS 1. Computer programs for analysis of fluid inclusion data and for modelling bulk fluid properties. Chemical Geology, *194*(1-3), 3-23.

Bodnar, R.J. (1993). Revised equation and table for determining the freezing point depression of H2O-NaCl solutions. Geochimica et Cosmochimica acta, 57(3), 683-684.

Bodnar, R.J. Lecumberri-Sanchez, P. Moncada, D. and Steele-MacInnis, M (2014). Fluid inclusions in hydrothermal ore deposits. Treatise on geochemistry, 13, 119-142.

Chattopadhyay, B, Chattopadhyay, S & Bapna, V.S (1994). Geology and geochemistry of Degana Pluton-a Proterozoic rapakivi granite in Rajasthan, India; Mineralogy and Petrology. 50, 69-82.

Darling, R.S. (1991). An extended equation to calculate NaCl contents from final clathrate melting temperatures in H_2O-CO_2-NaCl fluid inclusions: Implications for PT isochore location. Geochimica et Cosmochimica Acta, 55(12), 3869-3871.

Deng, J. Li, J. Zhang, D. Chou, I.-M. Yan, Q. Xiong.X. (2022). Origin of pegmatitic melts from granitic magmas in the formation of the Jiajika lithium deposit in the eastern Tibetan Plateau. Journal of Asian Earth Sciences, 229, 105147.

Frezzotti, M.L., Tecce, F. and Casagli, A., 2012. Raman spectroscopy for fluid inclusion analysis. Journal of Geochemical Exploration, 112, 1-20.

Ghosh, U. Upadhyay, D. Mishra, B. & Abhinay, K. (2023). In-situ trace element and Li-isotope study of zinnwaldite from the Degana tungsten deposit, India: implications for hydrothermal tungsten mineralization. Chemical Geology, 632, 121550.

Guo, J. Xiang, L. Zhang, R. Yang, T. Wu, K. Sun, W. (2022). Chemical and boron isotopic variations of tourmaline deciphering magmatic-hydrothermal evolution at the Gejiu Sn-polymetallic district South China Chemical Geology, 593, 120698.

Guo-Guang Wang. Fan-Bo Zheng. Pei Ni. Yan-Wei Wu. Wen-Xiang Qi. Zi-Ang Li. (2023). Fluid properties and ore forming process of the giant Jiajika pegmatite Li deposit, western China. Ore Geology Reviews, 160, 105613. https://doi.org/10.1016/j.oregeorev.2023.105613.

Heinrich, C.A. (1990). The chemistry of hydrothermal tin-tungsten ore deposition. Economic Geology, 85, 457-481.

Heinrich, C.A. Driesner, T. Stefansson, A. Seward, T.M. (2004). Magmatic vapor contraction and the transport of gold from the porphyry environment to epithermal ore deposits. Geology, 32(9), 761-764.

Huang, T. Fu, X. Ge, L. Zou, F. Hao, X. Yang, R. Xiao, R. & Fan, J. (2020). The genesis of giant lithium pegmatite veins in Jiajika, Sichuan, China: Insights from geophysical, geochemical as well as structural geology approach. Ore Geology Reviews, 124, 103557.

Hulsbosch, N. Hertogen, J. Dewaele, S. André, L. & Muchez, P. (2014). Alkali metal and rare earth element evolution of rock-forming minerals from the Gatumba area pegmatites (Rwanda): Quantitative assessment of crystal-melt fractionation in the regional zonation of pegmatite groups. Geochimica et Cosmochimica Acta, 132, 349-374.

Jolliff, B.L. Papike, J.J. & Shearer, C.K. (1987). Fractionation trends in mica and tourmaline as indicators of pegmatite internal evolution: Bob Ingersoll pegmatite, Black Hills, South Dakota. Geochimica et Cosmochimica Acta, 51(3), 519-534.

Kaeter, D. Barros, R. Menuge, J.F. & Chew, D.M. (2018). The magmatic-hydrothermal transition in rare-element pegmatites from southeast Ireland: LA-ICP-MS chemical mapping of muscovite and columbite-tantalite. Geochimica et Cosmochimica Acta, 240, 98-130.

Kumar, S. Bhardwaj, S. Sharma, A. & Sharma, V. (2023). W-Li Potentials in the Tailing Dumps of Rewat Hill, Degana, Rajasthan, NW India; Constraints from Petrography and Geochemistry. Journal of the Geological Society of India, 99(10), 1438-1444.

Li, B. Zhao, L. Lu, A.H. Luo, J.B. Kong, H. & Lai, J.Q. (2023). Mineralogical constraints on pegmatite genesis and rare metal mineralization in the Mufushan batholith, South China. Ore Geology Reviews, 105856.

Li, H. Cao, J. Thomas, J. Jiang, A.W. Liu, B. Wu, Q. (2019). Zircons reveal multi-stage genesis of the Xiangdong (Dengfuxian) tungsten deposit, South China, Ore Geology Reviews, 111. doi.org/10.1016/j.oregeorev.2019.102979

Li, J. Huang, X.L. Fu, Q. Li, W.X. (2021). Tungsten mineralization during the evolution of a magmatic-hydrothermal system: Mineralogical evidence from the Xihuashan rare-metal granite in South China. American Mineralogist, 106 (3), 443-460. https://doi.org/10.2138/am-2020-7514.

Linnen, R.L. Van Lichtervelde, M. & Černý, P. (2012). Granitic pegmatites as sources of strategic metals. Elements, 8(4), 275-280.

Liu, S. Wang, R. Jeon, H. Hou, Z. Xue, Q. Zhou, L. Chen, S. Zhang, Z. & Xi, B. (2020). Indosinian magmatism and rare metal mineralization in East Tianshan orogenic belt: An example study of Jingerquan Li-Be-Nb-Ta pegmatite deposit. Ore Geology Reviews, 116, 103265.

Pandian, M.S. (1999). Late Proterozoic acid magmatism and associated tungsten mineralisation in northwest India. Gondwana Research, 2(1), 79-87.

Pandian, M.S & Varma, O.P. (2001). Geology and geochemistry of topaz granite and associated wolframite deposit at Degana, Rajasthan. Journal of Geological Society of India, 57, 297-307.

Roedder, E. (1992). Fluid inclusion evidence for immiscibility in magmatic differentiation. Geochimica et Cosmochimica Acta, 56(1), 5-20.

Shearer, C.K. Papike, J.J. & Laul, J.C. (1987). Mineralogical and chemical evolution of a rare-element granite-pegmatite system: Harney Peak Granite, Black Hills, South Dakota, Geochimica et Cosmochimica Acta, 51(3), 473-486, https://doi.org/10.1016/0016-7037(87)90062-7

Shepherd, T.J., Rankin, A.H. and Alderton, D.H. (1985). A Practical Guide to Fluid Inclusion Studies. Blackie and Sons, 239.

Singh, S.K & Singh, S. (2001). Geochemistry and tungsten metallogeny of the Balda Granite, Rajasthan, India; Gondwana Research, 4, 487-495.

Sovacool, B.K. Ali, S.H. Bazilian, M. Radley, B. Nemery, B. Okatz, J. Mulvaney, D. (2020). Sustainable minerals and metals for a low-carbon future. Science, 367, 30-33.

Vijay Anand, S. Pandian, M. S. Balakrishnan, S. & Sivasubramaniam, R (2018). Fluid inclusion, geochemical, Rb-Sr and Sm-Nd isotope studies on tungsten mineralized Degana and Balda granites of the Aravalli craton, NW India. Journal of Earth System Science, 127, 1-20.

Wang, X.B. Ge, J.P. Li, J.S. Han, A.P (2017). Market impacts of environmental regulations on the production of rare earths: a computable general equilibrium analysis for China. Journal of Clean Production, 154 (2017), 614-620.

Wenkai, J. Xudong, C. Rucheng, W. Zhiqin, X. Huan, H. Rongqing, Z. Guangwei, L, Zheng, B. (2023). The deep rare metal metallogenic characteristics of the Jiajika lithium polymetallic deposit in Sichuan Province, China: Revealed by the Jiajika Scientific Drilling. Ore Geology Reviews, 160, 105579. https://doi.org/10.1016/j.oregeorev.2023.105579.

Xie, G. Mao, J. Li, W. et al. (2019). Granite-related Yangjiashan tungsten deposit, southern China. Mineralium Deposita, 54, 67-80. doi.org/10.1007/s00126-018-0805-5.

Xie, L. Tao, X. Wang, R. Wu, F. Liu, C. Liu, X. Li, X. & Zhang, R. (2020). Highly fractionated leucogranites in the eastern Himalayan Cuonadong dome and related magmatic Be-Nb-Ta and hydrothermal Be-W-Sn mineralization. Lithos, 354, 105286.

Xu, Z. Zheng, B. Zhu, W. Chen, Y. Li, G. Gao, J. Che, X. Zhang, R. Wei, H. Li, W. & Wang, G. (2023). Geologic scenario from granitic sheet to Li-rich pegmatite uncovered by Scientific Drilling at the Jiajika lithium deposit in eastern Tibetan Plateau. Ore Geology Reviews, 105636.

Xu, Z.Q. Zhu, W. Zheng, B. Shu, L.S. Li, G.W. Che, X.D. & Qin, Y.L. (2021). New energy strategy for lithium resource and the continental dynamics research-celebrating the centenary of the School of Earth Sciences and Engineering, Nanjing University. Acta Geologica Sinica, 95(10), 2937-2954.

Yin, R. Huang, X.L. Xu, Y.G. Wang, R.C. Wang, H. Yuan, C. Ma, Q. Sun, X.M. & Chen, L.L. (2020). Mineralogical constraints on the magmatic-hydrothermal evolution of rare-elements deposits in the Bailongshan granitic pegmatites, Xinjiang, NW China. Lithos, *352*, 105208.

Yin, R. Wang, R.C. Zhang, A.C. Hu, H. Zhu, J.C. Rao, C. & Zhang, H. (2013). Extreme fractionation from zircon to hafnon in the Koktokay No. 1 granitic pegmatite, Altai, northwestern China. American Mineralogist, 98(10), 1714-1724.

Zhang, J. Liu, X.X. Zeng, Z. Li, W. Peng, L. Hu, H. Cheng, J. Lu, K. (2021). Age constraints on the genesis of the Changkeng tungsten deposit, Nanling region, South China. Ore Geology Reviews, 134, 104-134. https://doi.org/10.1016/j.oregeorev.2021.104134.